

SYSTEMATICS OF CHARGED-PARTICLE PRODUCTS FROM REACTIONS INDUCED BY 95-MeV ${}^6\text{Li}$

S.E. Vigdor, C. Castaneda, H.J. Karwowski, P.P. Singh, H.A. Smith, and J.D. Wiggins

Energy and angular distributions of charged particles produced in collisions of 95-MeV ${}^6\text{Li}$ with ${}^{56}\text{Fe}$, ${}^{90}\text{Zr}$, and ${}^{197}\text{Au}$ have been investigated. The results can be compared with similar data obtained with heavier and with lighter ions, in order to see how the distribution of non-fusion reaction strength evolves with changing projectile mass.

A five-element silicon-detector telescope (front-counter thickness = 12 μm , total depth = 12 mm) allowed identification of products with $1 \leq Z \leq 15$ over the entire energy range of interest, and in addition of the high-Z, high-energy (up to ~ 90 MeV) fission fragments from ${}^6\text{Li} + {}^{197}\text{Au}$. Representative two-dimensional spectra (E_{total} vs. ΔE) are shown in Fig. 1. In the spectrum shown for ${}^6\text{Li} + {}^{197}\text{Au}$ the ΔE_1 gain has been reduced sufficiently to illustrate the clean separation of the fission fragments from all other reaction products. Typical total-energy spectra for $Z = 1$ and $Z = 2$ products are shown in Fig. 2. In Fig. 3 we show angular distributions of various reaction products from ${}^6\text{Li} + {}^{90}\text{Zr}$ over the angular range for which the data have been reduced to date. Reduction of data for ${}^{90}\text{Zr}$ at larger angles, and for the other targets, is still in progress.

The energy spectra for $Z = 1$ and $Z = 2$ (Fig. 2) show evidence of compound-nucleus evaporation (the low-energy p and α peaks), of fragmentation of the ${}^6\text{Li}$ (beam-velocity peaks for p, d, and α), and of pre-equilibrium emission (most clearly seen in the proton spectrum "tail" above 20 MeV). Although

the prominence of the beam-velocity peaks clearly reflects the loosely bound α -d or α -p-n structure of ${}^6\text{Li}$ (the ${}^3\text{He}$ -t configuration being much more tightly bound), it is not yet clear how much of this strength corresponds to essentially two-body final states, as opposed to direct multi-body break-up -- this question is the subject of further investigation (experiment #43).

The energy spectra for ${}^6,7\text{Li}$ and ${}^7\text{Be}$ products (not shown) exhibit features expected for simple direct reactions: the strength is overwhelmingly concentrated at low excitation energies ($E_x \lesssim 10$ MeV) in relatively few, strongly excited states. These spectra all exhibit a flat but very weak tail extending to low energies. Products heavier than ${}^7\text{Be}$ are produced quite weakly, predominantly at low energies ($E_{\text{lab}} \approx 15\text{-}30$ MeV), and perhaps in part from slight oxygen or carbon contamination of the targets. The angular distributions shown for the heavy products in Fig. 3a correspond to summation of all events with outgoing energies above ($B-10$ MeV), where B is the calculated Coulomb barrier for a two-body exit channel.

There is some correlation between the energy of the detected particles and the steepness of the forward peak in the corresponding angular distribution, similar to effects seen with heavier projectiles. Thus, the most sharply forward-peaked distributions in Fig. 3a correspond to the channels dominated by inelastic scattering or single-nucleon

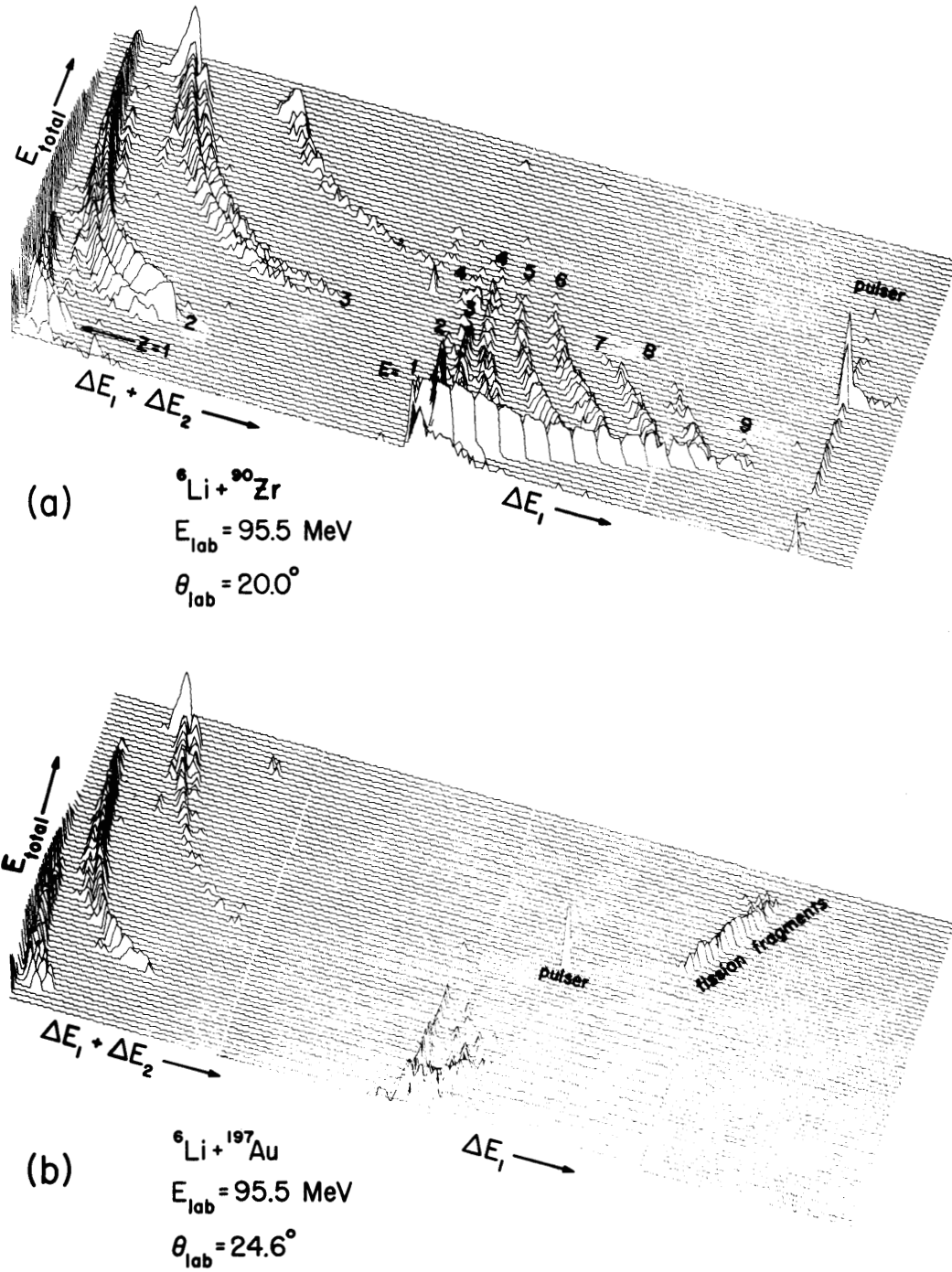


Fig. 1. Representative two-dimensional spectra obtained with the five-element charged-particle telescope. The left half of each plot shows E_{total} vs. $(\Delta E_1 + \Delta E_2)$ for only those particles which progress at least as far as the third detector in the stack; the right half-plane shows E_{total} vs. ΔE_1 for those particles which stop in the first or second detector. The ΔE_1 gain in (b) has been reduced by a factor of ~ 4 relative to (a) in order to display the fission fragments detected for ${}^6\text{Li} + {}^{197}\text{Au}$. The vertical (counts) scale is logarithmic.

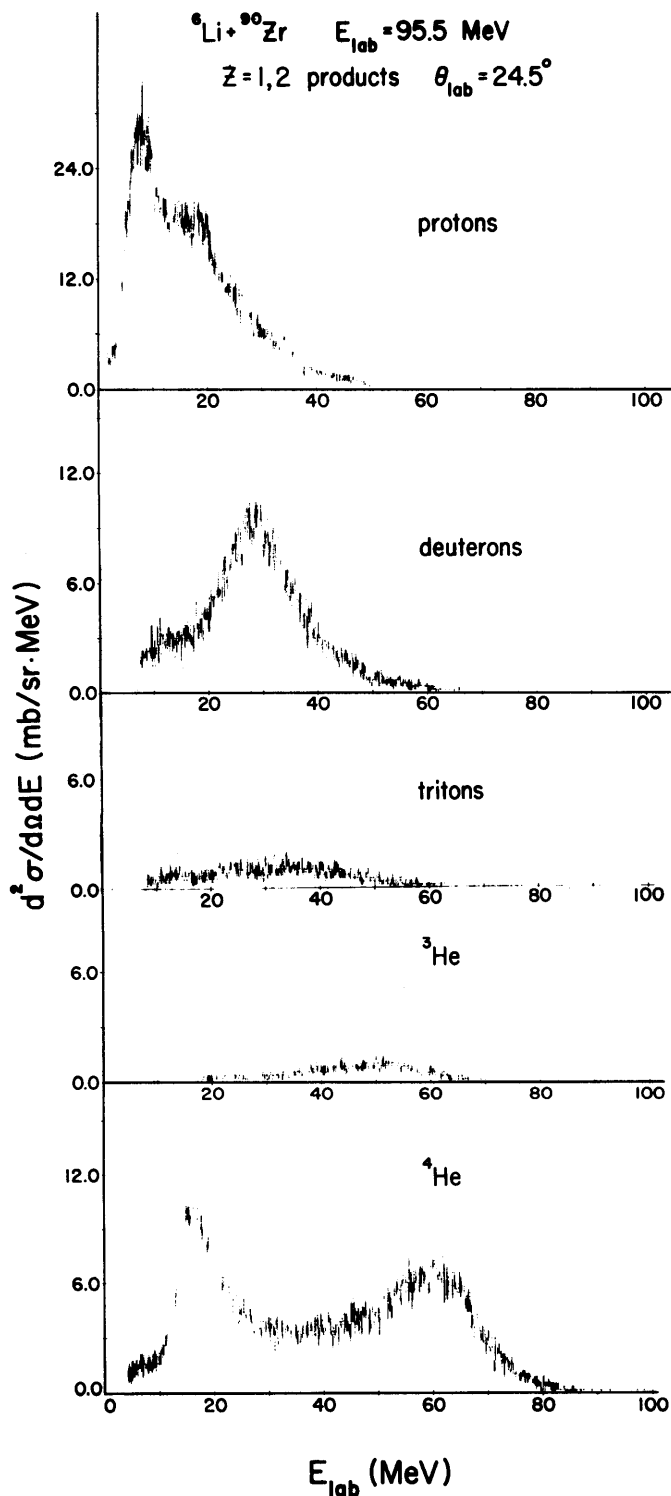


Fig. 2. Typical total-energy spectra obtained for $Z = 1$ and $Z = 2$ products for ${}^6\text{Li} + {}^{90}\text{Zr}$.

transfer to low-lying states. This correlation is also seen in Fig. 3b, where the angular distributions for inclusive α -production are observed to remain sharply forward-peaked over the entire extent of the beam-velocity peak, but then to flatten gradually in the region intermediate between the beam-velocity and evaporation peaks. The strength in this "transition" region of the α -spectrum cannot be explained simply by the overlap of the two prominent peaks, and arises presumably from reactions of time scale intermediate between the direct and compound-nucleus mechanisms responsible for the peaks.

The angular distribution of the fission fragments from ${}^6\text{Li} + {}^{197}\text{Au}$ is symmetric about $\theta_{\text{cm}} = 90^\circ$, indicative of equilibrium fission, with a small deviation from isotropy (i.e., from $d\sigma/d\Omega \propto 1/\sin\theta_{\text{cm}}$). The measured total fission cross section is $\sigma_{\text{fiss}} = (219 \pm 20)\text{mb}$. This result is consistent with the range of possible predicted fission cross sections (using codes ALICE¹ and MB-II², and rotating-liquid-drop model fission barriers) only if the great majority of partial waves participating in reactions lead to compound-nucleus formation. (The grazing ℓ -value for 95-MeV ${}^6\text{Li} + {}^{197}\text{Au} \approx 50 \hbar$). An intensive study of the distribution of strength among all decay modes of high-spin compound nuclei formed in fusion of ${}^6\text{Li}$ with heavy rare-earth target nuclei will be undertaken in a future experiment.

The results of this experiment analyzed to date allow the following conclusions. (1) We see no evidence for significant clustering of strength near the exit-channel Coulomb-repulsion energies

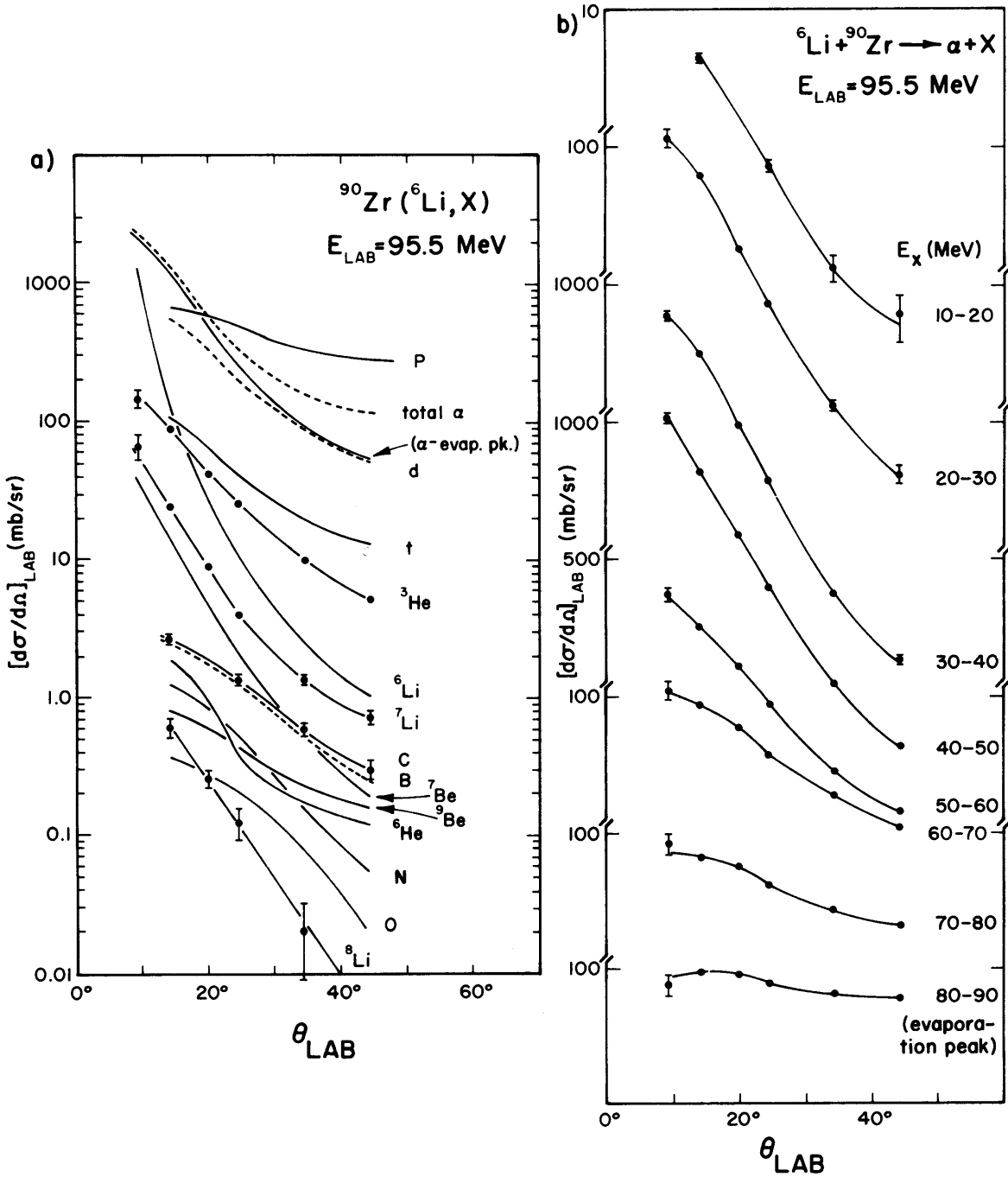


Fig. 3. a) Energy-integrated angular distributions for various charged-particle products from ${}^6\text{Li} + {}^{90}\text{Zr}$. Smooth curves drawn through the measurements are shown, with the actual data indicated for a few representative channels. (b) Evolution of the measured angular distributions for inclusive α -production in ${}^6\text{Li} + {}^{90}\text{Zr}$, as a function of the equivalent excitation energy (E_x) which would be associated with a two-body exit channel.

(except, of course, in the evaporation peaks); thus, "deeply inelastic" processes, akin to those observed for heavier projectiles at comparable energies per nucleon, do not seem important here. This observation is consistent with the suggestion from elastic scattering results³ that there is a transition in the nature of the absorption mechanisms between ${}^6\text{Li}$ and ${}^{12}\text{C}$ projectiles. (2) There is, for all three target nuclei, a sizeable total direct-reaction cross section (~ 0.5 -1 barn), which is dominated by "breakup-like" processes characteristic of the loosely bound internal structure of ${}^6\text{Li}$. (3) The only significant strength observed for processes intermediate between direct and compound-nucleus mechanisms is in the $Z=1$ and $Z=2$ spectra, e.g., the "transition" region of the α -spectrum. It is not yet clear if

this strength in the α -spectrum is influenced by the presence of loosely bound α 's in the projectile, or if it is more generally characteristic of the pre-equilibrium decay of highly excited composite systems.

- 1) M. Blann and F. Plasil, ALICE: A Nuclear Evaporation Code, U.S.A.E.C. Report No. C00-3493-10 (1973, unpublished).
- 2) M. Beckerman and M. Blann, MB-II: A Statistical Fission/Evaporation Code, University of Rochester Nuclear Structure Research Laboratory Report No. URNSRL-135A (1977, unpublished).
- 3) R.M. DeVries, D.A. Goldberg, J.W. Watson, M.S. Zisman, and J.G. Cramer, Phys. Rev. Letters 39, 450 (1977).